CrystEngComm

Cite this: *CrystEngComm*, 2012, **14**, 6492–6502

www.rsc.org/crystengcomm

PAPER

Supramolecular patterns of cationic and neutral Ni(II) complexes from the interplay of hydrogen-bonding, stacking interactions and metal-coordination motifs†

Konstantina A. Kounavi,[a] Eleni E. Moushi,[b] Manolis J. Manos,[b] Constantina Papatriantafyllopoulou,[a] Anastasios J. Tasiopoulos[b] and Vassilios Nastopoulos*[a]

Received 7th May 2012, Accepted 22nd June 2012
DOI: 10.1039/c2ce25704a

In an effort to explore the way in which the chemical subunits of crystal structures of transition metal complexes are put together in periodic ordered arrays in the solid state *via* noncovalent interactions, an investigation on a series of 13 nickel(II) complexes has been carried out. The complexes were isolated from the general $Ni^{II}/X^-/L$ or HL′ [X^- = Cl^-, Br^-, I^-, NO_3^-, NO_2^-, ClO_4^-; L = 1-methyl-4,5-diphenylimidazole, and HL′ = 4,5-diphenylimidazole] reaction system. A single-crystal diffraction analysis shows that, independently of the ligand used, most of the complexes contain the rigid square planar $[NiL_4]^{2+}$ (**1–5**) or $[Ni(HL')_4]^{2+}$ (**6–10**) cation, which seems to have an impact on the self-assembly process by adopting a structure-directing role: the supramolecular assembly is organized around the rigid bulky cations *via* interactions with the surrounding counterion/solvent clusters in each individual structure. The components of the clusters, *i.e.* OH^-/H_2O (**1**), $[NiCl_4]^{2-}$/EtOH (**2**), Br^-/H_2O (**3**), NO_3^-/MeOH (**4**), ClO_4^-/Me_2CO (**5**), Cl^-/H_2O (**6**), Br^-/MeCN (**7**), $I^-/Me_2CO/H_2O$ (**8**), NO_3^-/EtOH/H_2O (**9**), and ClO_4^-/Me_2CO (**10**), are held tightly together by strong or weak hydrogen bonding. The structure-directing action of the cations is accomplished *via* weak C–H···O/Cl/Br^-, π···π and C–H···π interactions (for L-containing complexes) or strong recurring N–H···/Cl^-/Br^-/I^-/O motifs dominating the molecular self-assembly together with weak interactions (for HL′-containing complexes). The variety of the stereochemistries observed among the studied compounds (square planar, **1–10**; tetrahedral, **11** and **12**; octahedral, **13**) seems to advocate the choice of nickel as an interesting candidate in metallosupramolecular research.

Introduction

The rational design and preparation of supramolecular assemblies through the coordination of metal ions with organic ligands has attracted attention for developing novel crystalline materials with interesting structural topologies and promising applications, and has evolved an interesting research field termed as metallosupramolecular chemistry.[1] The metals used in these complexes can serve as structural components and/or as a source of properties (*e.g.*, magnetic, catalytic, optoelectronic, *etc*). The two most commonly used approaches for engineering the crystal structure of such complexes employ either coordination bonds[2] or supramolecular interactions.[3] Both approaches and their combinations have resulted in the construction of pre-designed high-dimensional supramolecular architectures. The coordination bond as a supramolecular synthon[4] has been widely studied in recent decades (catenanes, rotaxanes, molecular knots, coordination polymers, metal–organic frameworks, *etc*). The hydrogen bonds[5] are the most common directing forces on the self-assembly process of individual molecules due to their relative strength, directionality and ability to act synergically. At the same time, the significance of other motifs such as π···π interactions,[6] a class of weak non-directional forces found in both natural and synthetic systems, should not be underestimated in the context of crystal engineering. Studies on such interactions have mainly focused on organic systems, while transition metal complex systems are somewhat less explored.

Among other transition metals, nickel has played an important role in the development of modern inorganic chemistry.[7,8] The chemistry of Ni features a very wide variety of mono- and polydentate ligands, with metal oxidation states ranging from 0 to +V, although organometallic Ni^{-I} and Ni^{-II} species have been reported. The most common oxidation state by far is Ni^{II}. The coordination chemistry of Ni(II) has flourished since 1980, stimulated by, *inter alia*, the discovery and mechanism of action of the enzyme urease, the use of complexes in catalysis and the

[a]*Department of Chemistry, University of Patras, Patras, 26504, Greece. E-mail: nastopoulos@chemistry.upatras.gr*
[b]*Department of Chemistry, University of Cyprus, Nicosia, 1678, Cyprus*

† Electronic supplementary information (ESI) available: Molecular overlay figures, additional drawings, IR spectra and tables with hydrogen-bonding geometries. CCDC reference numbers 881062–881074. For ESI and crystallographic data in CIF or other electronic format see DOI: 10.1039/c2ce25704a

booming interest in Ni^{II}-containing materials with specific properties related to magnetism and nonlinear optics.[7] By contrast with the molecular chemistry of Ni(II), the supramolecular chemistry of this metal ion has received scant attention. Nickel(II) has certain characteristics that might prove valuable for the development of its supramolecular chemistry. It forms a large number of complexes with coordination numbers 3 to 6.[9] Being a d^8 system, it shows an exceptional preference for octahedral as opposed to tetrahedral coordination with weak-field ligands, due to the large Crystal Field Stabilization Energy (CFSE) for the former geometry.[10] Bulky weak-field ligands often give tetrahedral complexes, whereas medium-field bulky or strong-field ligands favour square planar coordination; the latter is a natural consequence of the d^8 configuration, since the planar ligand set causes one of the *d* orbitals ($d_{x^2-y^2}$) to be uniquely high in energy and the eight electrons can occupy the other four *d* orbitals leaving this strongly antibonding one vacant. Ni(II) also has a tendency to add a further ligand to give 5-coordinate species, both trigonal bipyramidal and square pyramidal depending on the present and/or the incoming fifth ligand. Another particular characteristic[9] of its chemistry is the existence of complicated equilibria in solution, commonly temperature- and concentration-dependent, and this sometimes gives different structural types (formation of 4-, 5- and 6-coordinate complexes, monomer-polymer formation, planar-tetrahedral complex formation, unusual isomerism) in the solid state even with the same set of ligands. All the above mentioned *molecular* characteristics of Ni(II) complexes can lead to interesting *supramolecular* features, *e.g.* formation of 1D, 2D or 3D networks formed by hydrogen bonding and/or π···π stacking interactions and supramolecular isomerism, amongst others. It is thus obvious that the choice of organic and inorganic ligands is not only important in the classical (molecular) coordination of Ni(II), but it is also crucial in the development of its metallosupramolecular chemistry.

In this context we have designed and prepared a series of Ni^{II} complexes using as ligands two substituted imidazoles, 1-methyl-4,5-diphenylimidazole (L) and 4,5-diphenylimidazole (HL′), coordinated to the metal ion *via* the pyridine-type N3 atom (Scheme 1). Imidazole and its derivatives are, among others, particularly interesting ligands in bioinorganic[11,12] and metallo-supramolecular[13] chemistry. The ligands employed have the following features: (i) Both have two phenyl rings which, combined with the π-excessive character of the 5-membered heterocyclic ring, can form π···π interactions, (ii) ligand HL′, in contrast to L, has a hydrogen-bond donor (the pyrrolic-type N1 atom) enabling the formation of recurring intermolecular units (supramolecular packing motifs or synthons) that can potentially assist the molecular self-assembly, and (iii) they have similar molecular structures, hence comparative studies of the inter-molecular organization of their complexes is easier. There has been relatively little work on the coordination chemistry of heavily substituted imidazoles, and in particular about L[14–18] and HL′.[18,19] The ions X^- (X^- = Cl^-, Br^-, I^-, NO_3^-, NO_2^-, ClO_4^-) used were selected on the basis of (i) their tendency to act as monodentate terminal ligands,[16,18] thus avoiding the isolation of coordination polymers, (ii) their ability to coordinate or act as counterions:[18,20] neutral and cationic complexes were expected, respectively, and (iii) their size,[21] in order to study their effect on the complex stoichiometry (when coordinated) or their role in the supramolecular organization process as counterions. Strong basic counterions, *e.g.* $MeCO_2^-$ ions, gave strong evidence of ligand deprotonation in the case of HL′ and formation of polymeric species.

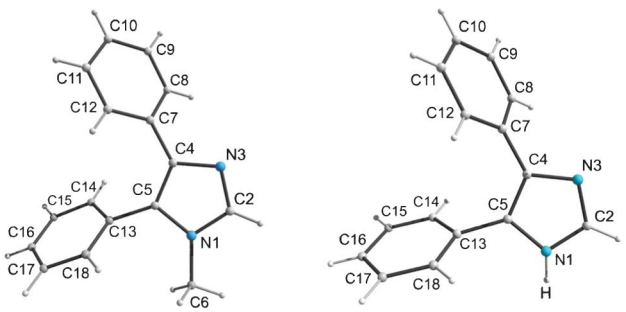

Scheme 1 The monodentate ligands L (left) and HL′ (right).

We report here the results of this approach: a total of 13 new Ni(II) complexes (**1–13**) have been prepared and characterized. The methodology used comprises reactions of simple Ni(II) salts (NiX_2) with the L and HL′ ligands; the parameters studied include the nature of X^-, the reaction solvent, the molar ratio of reagents, the crystallization solvent, and the crystallization method. In each group of experiments we tried to vary one parameter at a time in order to isolate the maximum number of products for a given reaction system. The structural analysis indicated the tendency of the Ni(II) centres to form square planar $[NiL_4]^{2+}$ and $[Ni(HL')_4]^{2+}$ cations (**1–10**) adopting a structure-directing role in the supramolecular organization of the corresponding complexes, while the tetrahedral (**11**, **12**) and octahedral (**13**) stereochemistries also observed among the prepared compounds seem to advocate the choice of nickel as an interesting candidate in metallosupra-molecular research.

Results and discussion

Synthetic comments

A multitude of reactions have been systematically explored with differing reagent ratios, reaction solvents, hydro(solvo)thermal techniques, and other conditions aimed at preparing the largest possible number of Ni(II) complexes of L and HL′ ligands. In some cases triethylorthoformate (TEOF) was added as a drying agent. Ni(II) is air-stable, therefore the synthetic work was conducted in the normal laboratory atmosphere; furthermore it is located on the right of the Irving–Williams series, ensuring significant thermodynamic stability for its complexes, a key issue in crystal engineering. The general synthetic route with the individual formulae of the complexes is illustrated in Scheme 2. In each case, the crystalline product was characterized by IR spectroscopy, microanalysis, and single-crystal X-ray diffraction. Complexes **1–10** were obtained by reactions with metal-to-ligand ratio of 1 : 2.5 up to 1 : 4 with a square planar geometry for the metal centre; however, by changing the ratio to 1 : 1, the reactions resulted in complexes **11–13** with tetrahedral and octahedral geometries. Reactions with an excess of Ni^{II} did not affect the product identity.

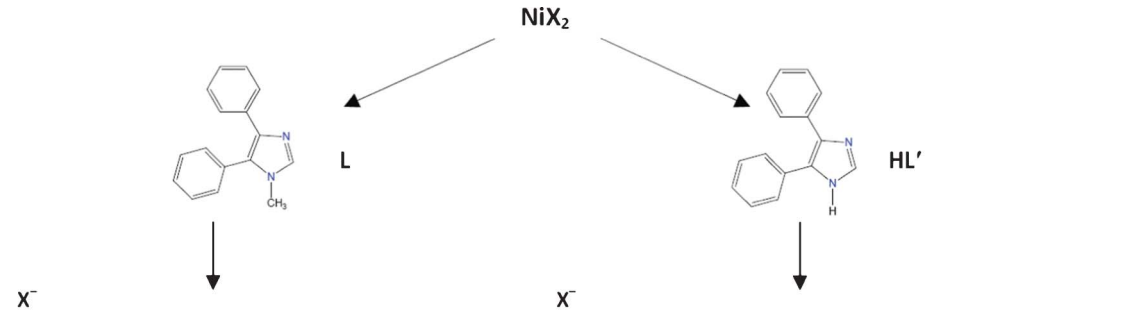

X⁻			X⁻		
Cl^-	$[NiL_4](OH)_2{\cdot}H_2O$	**1**·H_2O	Cl^-	$[Ni(HL')_4][NiCl_2(HL')_2]_2Cl_2{\cdot}1.35H_2O$	**6**·$1.35H_2O$
Cl^-	$[NiL_4][NiCl_4]{\cdot}2EtOH$	**2**·2EtOH	Br^-	$[Ni(HL')_4]Br_2{\cdot}4.7MeCN$	**7**·4.7MeCN
Br^-	$[NiL_4]Br_2{\cdot}3.4H_2O$	**3**·$3.4H_2O$	I^-	$[Ni(HL')_4]I_2{\cdot}2Me_2CO{\cdot}0.8H_2O$	**8**·$2Me_2CO{\cdot}0.8H_2O$
NO_3^-	$[NiL_4](NO_3)_2{\cdot}2.8MeOH$	**4**·2.8MeOH	NO_3^-	$[Ni(HL')_4](NO_3)_2{\cdot}2EtOH{\cdot}2H_2O$	**9**·$2EtOH{\cdot}2H_2O$
ClO_4^-	$[NiL_4](ClO_4)_2{\cdot}Me_2CO$	**5**·Me_2CO	ClO_4^-	$[Ni(HL')_4](ClO_4)_2{\cdot}2.8Me_2CO$	**10**·$2.8Me_2CO$
Cl^-	$[NiCl_2L_2]$	**11**			
Br^-	$[NiBr_2L_2]$	**12**			
NO_2^-	$[Ni(NO_2)_2L_2]$	**13**			

Scheme 2 General synthetic route for the Ni(II) compounds with ligands L and HL′.

Description of the structures of complexes 1–5

$[NiL_4]X_2$ type complexes. *Note*: To facilitate discussion, molecular comparison and overlay, the same numbering scheme has been assigned (where applicable) to the ligand atoms (Scheme 1), the coordinated ions, and the counterions/solvents for all compounds presented herein.

This group comprises complexes with X^- = OH^- (**1**), ½$[NiCl_4]^{2-}$ (**2**), Br^- (**3**), NO_3^- (**4**) and ClO_4^- (**5**). Repeated attempts to isolate the anticipated compound $[NiL_4]I_2{\cdot}$solvent yielded only an amorphous material making it impossible to characterize crystallographically. We observe that the structures of **1** (isolated by hydrothermal conditions) and **2** contain as counterions OH^- and $[NiCl_4]^{2-}$, respectively, instead of the expected Cl^- (Scheme 2). A common feature in all five structures is the presence of the $[NiL_4]^{2+}$ cation (Fig. 1) in which the metal is coordinated through the pyridine-type nitrogen donor atom from each of the four ligands, resulting in a NiN_4 square planar geometry. This coordination is in accordance with the principles of the CFSE theory for Ni(II) complexes, given that L is a medium-field ligand. The asymmetric unit of compounds **1**, **2** and **3** contain half a $[NiL_4]^{2+}$ cation (Z' = ½), the other half generated by a C_2 axis lying on the NiN_4 equatorial plane and passing through the metal centre. Nevertheless, Ni^{II} is not in a perfectly square planar geometry due to lack of D_{4h} (4/*mmm*) symmetry in the coordination environment of the nickel ion, as evidenced by the N–Ni–N values (close to 90°) of the NiN_4 group. In all cases (**1–5**), the cation's ligands are combined into two pairs; within each pair the two ligands are mutually accommodated in a *syn* fashion and in an "antiparallel" way with their methyl groups pointing at opposite directions. This arrangement favors the formation of two intramolecular π···π stackings in each pair of ligands, providing considerable rigidity to the $[NiL_4]^{2+}$ cations (Fig. 1). Similar π···π motifs have been encountered in a few previously characterized complexes with L,[15–18] supporting its utility as a crystal engineering tool. The conformation similarity among the $[NiL_4]^{2+}$ cations is highlighted in Fig. S1 (ESI†) showing the overlay of the cation pairs. As reasonably expected, the largest deviations occur in the region of the phenyl rings not involved in intramolecular π···π interactions, probably to comply with packing requirements. The r.m.s.d. values for the four pairs of cations (**1** being the reference molecule) are: 0.360 Å (**1**, **2**), 0.039 Å (**1–3**), 0.466 Å (**1–4**), and 0.153 Å (**1–5**).

The packing of compounds **1–5** discloses a characteristic mode of organization, common in all five compounds: the supramolecular

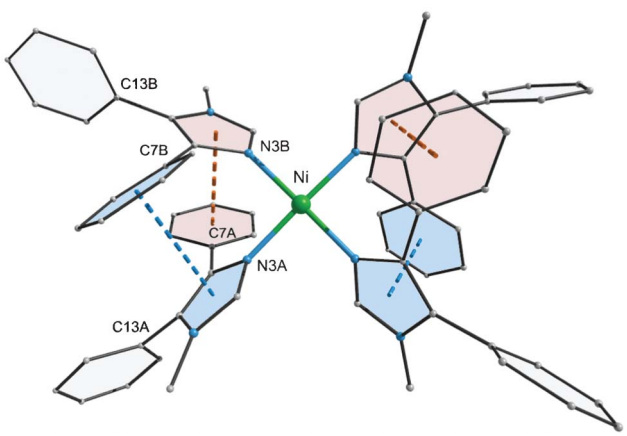

Fig. 1 The $[NiL_4]^{2+}$ cation of compound **1** with the four intramolecular π···π motifs ($d_{\pi\cdots\pi}$ = 3.577 Å for the blue pairs and 3.498 Å for the brown pairs). Hydrogen atoms have been omitted.

assembly is essentially organized around the $[NiL_4]^{2+}$ cations *via* weak C–H···X interactions (X = O, Cl, Br^-) with the surrounding counterion/solvent molecules. The latter are grouped in discrete clusters [OH^-/H_2O (**1**), $[NiCl_4]^{2-}$/EtOH (**2**), Br^-/H_2O (**3**), NO_3^-/MeOH (**4**) and ClO_4^-/Me_2CO (**5**)] with their components held firmly together *via* strong (compounds **1**, **2**, **3** and **4**) or weak (compound **5**) hydrogen bonding. In this way, the $[NiL_4]^{2+}$ cations adopt a structure-directing role resulting in 3D architectures for compounds **2**, **3**, **4** and **5**. As a representative example, the structure of compound **4** is given in Fig. 2. Compound **1** can only form 2D layers due to a lack of interactions between the $[NiL_4]^{2+}$ and the OH^- ions of neighbouring layers, probably due to the small size of the latter ions (Fig. S2, ESI†). A detailed survey of all interactions and structural motifs that contribute to the supramolecular self-assembly of the compounds is given in Table 1. Despite the large number of ligand π-systems in the cations of compounds **1–5**, no intermolecular π···π interactions have been identified, due to the buffering action of the intervening clusters. However, weak intermolecular C–H···π contacts[22] add, in most cases, to the stability of the resulting crystal structures. The coordination geometry of Ni^{II} in compound **2** is square planar in the $[NiL_4]^{2+}$ cations and tetrahedral in the $[NiCl_4]^{2-}$ counterions, the chloride ions being weak-field ligands in the latter case.

Description of the structures of complexes 6–10

$[Ni(HL')_4]X_2$ type complexes. This group includes compounds **6–10** with X^- = Cl^- (**6**), Br^- (**7**), I^- (**8**), NO_3^- (**9**) and ClO_4^- (**10**). Interestingly, the $[Ni(HL')_4]^{2+}$ cation is again a permanent component in all structures, with a distorted square planar coordination and stabilized by the same intramolecular π···π motif as in compounds **1–6**. The conformation similarity between the $[NiL_4]^{2+}$ and $[Ni(HL')_4]^{2+}$ cations in compounds **1–5** and **6–10**, respectively, is reflected in the overlays in Fig. S1, ESI.† At the supramolecular level, however, the presence of the N1–H group in ligand HL′, capable of directing strong hydrogen-bond motifs, provides additional tools for supramolecular self-assembly while increasing system complexity. The counterion/solvent species of each structure are, similarly to compounds **1–5**, organized into clusters, providing the appropriate acceptors (Cl, O, Br, I) to generate strong hydrogen bonding with the N1–H donors of the rigid $[Ni(HL')_4]^{2+}$ cations. The resulting 3D structures are further reinforced by weak interactions, depending on the composition, shape and size of the cluster in each individual structure. It has been shown that the inclusion of water in organic and metal–organic structures is of fundamental and practical importance.[23,24] Due to its very small size and excellent hydrogen-bonding ability, it can be hosted in many locations and environments. Indeed, the water molecules in compounds **1**, **3**, **6**, **8** and **9** form in all cases discrete clusters with the corresponding counterions, thus contributing to the self-assembly process of the crystalline structures, rather than being innocuous bystanders within the crystals.[24]

In particular, the asymmetric unit of compound **6**, a rather unexpected product isolated by hydrothermal conditions, also contains two tetrahedrally coordinated $[NiCl_2(HL')_2]$ molecules. In terms of cluster organization, disordered chloride counterions and solvent water molecules close to an inversion centre sum up with their symmetry-related counterparts into a tight Cl^-/H_2O cluster. A second chloride counterion acts as a multihydrogen-bonded acceptor. Thus, donors (N–H) and acceptors (Cl^-, O) co-operate *via* N–H···Cl^-/O hydrogen bonding towards a 3D assembly (geometry details in Table S1, ESI†). To accommodate, where appropriate, the formation of the dominant N–H···Cl^-/O patterns and/or minimize steric hindrance, the two $[NiCl_2(HL')_2]$

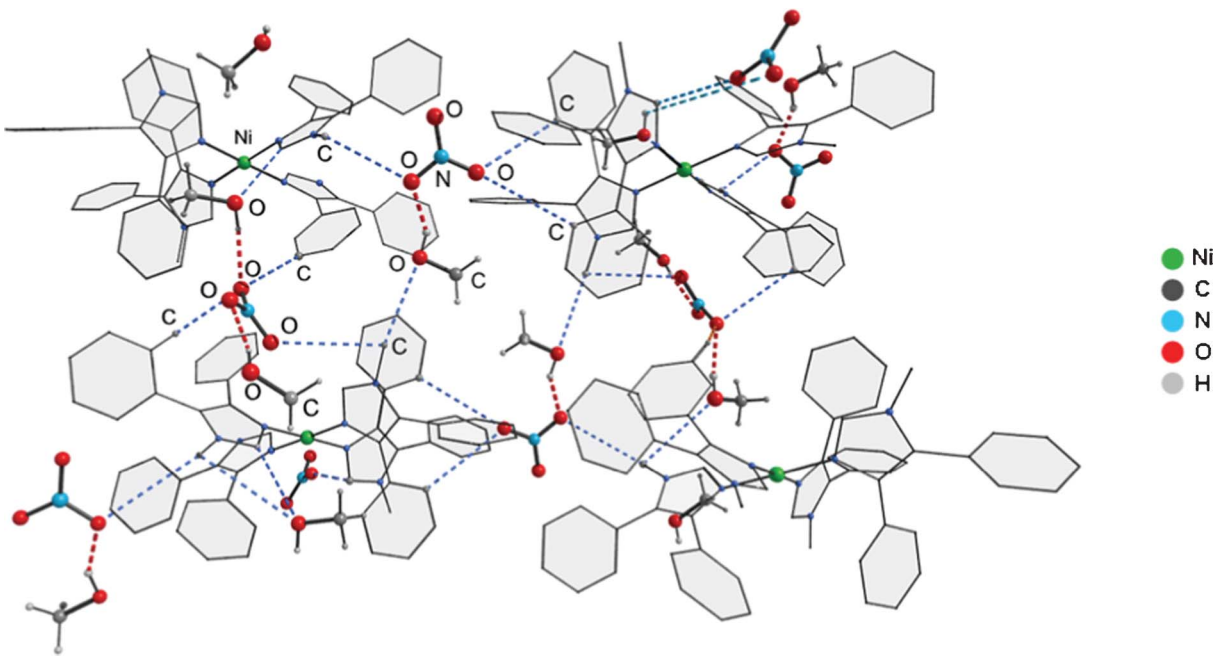

Fig. 2 A slab of the 3D structure of compound **4** showing the self-assembly of the NO_3^- counterions with the MeOH solvent molecules in discrete clusters (red dashed lines). The clusters are arranged around the $[NiL_4]^{2+}$ cations *via* weak C–H···O interactions (blue dashed lines). Hydrogen atoms (except those of the MeOH) have been omitted.

Table 1 Summary of all intra/intermolecular interactions observed in the crystal structures of the studied compounds **1–13**

Compound	Coordination geometry	Counterion + solvent clusters	Weak H-bonds	Strong H-bonds	Intra π···π	Inter π···π	Network
1·H_2O		$2(OH^-)/H_2O$	C–H···$O_{(OH^-)}$ C–H···π	O(H_2O)–H···$O_{(OH^-)}$	4	—	2D
2·2EtOH [a]		$[NiCl_4]^{2+}$/2EtOH	C–H···Cl C–H···O	O–H···Cl	4	—	3D
3·3.4H_2O		$2Br^-/3.4H_2O$	C–H···Br^- C–H···O C–H···π	O–H···Br^-	4	—	3D
4·2.8MeOH		NO_3^-/2MeOH NO_3^-/0.8MeOH	C–H···$O_{(H_2O)}$ C–H···$O_{(NO_3^-)}$ C–H···π	$O_{(MeOH)}$–H···$O_{(NO_3^-)}$	4	—	3D
5·Me_2CO		$2(ClO_4^-)/Me_2CO$	C–H···$O_{(ClO_4^-)}$ C–H···$O_{(Me_2CO)}$ $C_{(Me_2CO)}$–H···$O_{(ClO_4^-)}$ C–H···π	—	4	—	3D
6·1.35H_2O [b]		Cl^-/H_2O Cl^-, 0.35H_2O	C–H···Cl^- C–H···$Cl_{[NiCl_2(HL')_2]}$	**N–H···Cl$^-$** [c] **N–H···O** O–H···Cl^-	4 1 [d] 1 [d]	2	3D
7·4.7MeCN	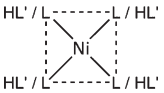	$2Br^-/4.7MeCN$	C–H···Br^- C–H···$N_{(MeCN)}$ C–H···π	**N–H···Br$^-$** N–H···$N_{(MeCN)}$	4	—	3D
8·2Me_2CO·0.8H_2O		$2I^-/2Me_2CO/0.8H_2O$	C–H···I^- $C_{(Me_2CO)}$–H···I^- C–H···$O_{(Me_2CO)}$	**N–H···I$^-$** $O_{(H_2O)}$–H···I^-	4	—	3D
9·2EtOH·2H_2O		$2(NO_3^-)/2H_2O$/2EtOH	C–H···$O_{(H_2O)}$ C–H···$O_{(NO_3^-)}$ C–H···$O_{(EtOH)}$ C–H···π	**N–H···O$_{(NO_3^-)}$** $O_{(H_2O)}$–H···$O_{(NO_3^-)}$	4	—	3D
10·2.8Me_2CO		$2(ClO_4^-)/2.8Me_2CO$	C–H···$O_{(ClO_4^-)}$ C–H···$O_{(Me_2CO)}$ $C_{(Me_2CO)}$–H···$O_{(ClO_4^-)}$ C–H···π	**N–H···O$_{(ClO_4^-)}$**	4	—	3D
11	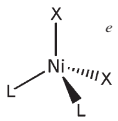 [e]	—	C–H···Cl C–H···π	—	2	2	3D
12		—	C–H···Br C–H···π	—	2	—	3D
13	 [f]	—	C–H···O C–H···N C–H···π	—	—	—	2D

[a] Tetrahedral coordination for the $[NiCl_4]^{2-}$ complex. [b] Tetrahedral coordination for the $[NiCl_2(HL')_2]$ complexes. [c] Supramolecular synthons are in bold. [d] Intramolecular π···π stacking in the $[NiCl_2(HL')_2]$ complexes. [e] X = Cl, Br. [f] represents the bidentate chelating nitrito ligand.

molecules are not, as would be expected, heavily involved in π···π stacking, nor do they retain the same conformation. In fact, one intramolecular π···π stacking is observed in each $[NiCl_2(HL')_2]$, while one of the latter molecules forms dimers with its centrosymmetric partner *via* two intermolecular π···π stackings (Table 1). The crystal packing is further supported *via* weak intermolecular C–H···Cl contacts.

The $[Ni(HL')_4]^{2+}$ cations of compound **7** are linked by lattice Br^- ions into chains along the *a* axis *via* strong N–H···Br^- motifs (Fig. 3, left). The chains are then connected by $2Br^-/4.7MeCN$ clusters into sheets parallel to the *ab* plane *via* N–H···Br^- and N–H···N_{MeCN} bonding; weak C–H···Br^- and C–H···π interactions connect the sheets into the final 3D structure. In compound **8**, the large radius of the iodide ions allow the direct formation of layers (rather than chains as in **7**) of $[Ni(HL')_4]^{2+}$ cations *via* N–H···I^- patterns (Fig. 4), the involved iodides belonging to $2I^-/2Me_2CO/0.8H_2O$ clusters. The 3D network is completed by C–H···I^- and acetone-mediated weak interactions (Table 1). No C–H···π interactions have been detected, owing to the large separation of the $[Ni(HL')_4]^{2+}$ cations.

The $[Ni(HL')_4]^{2+}$ cations of compound **9** are surrounded by $2(NO_3^-)/2H_2O$/2EtOH rigid clusters located around the C_2 axes of the structure. Its crystal structure is similar to **7**; however, the cations are connected in tapes *via* strong N–H···$O_{NO_3^-}$ motifs (Fig. 3, right). The tapes are linked in layers, and the layers are further expanded in a 3D network *via* weak C–H···O and C–H···π interactions. The crystal structure of compound **10** resembles that of **8**, *i.e.* layers are formed by strong N–H···$O_{ClO_4^-}$ motifs and subsequent expansion to 3D is achieved *via* weak intermolecular interactions (Table 1). It emerges therefore from the structures of **6–10** that the interaction of the rigid $[Ni(HL')_4]^{2+}$ building blocks through recurring N–H···X (X = Cl^-, Br^-, I^-, O) hydrogen-bonding motifs (acting as supramolecular synthons) is a dominating factor in the process of their supramolecular organization.

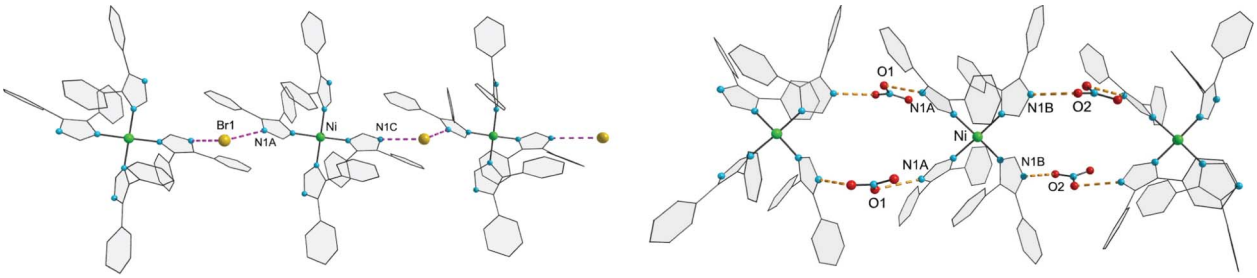

Fig. 3 (Left) Chains in the crystal structure of compound **7** formed by the $[Ni(HL')_4]^{2+}$ cations and the lattice Br^- ions *via* strong N–H···Br^- motifs. (Right) The cations and the nitrate ions of the surrounding rigid clusters in the structure of **9** are connected in tapes *via* strong N–H···$O_{NO_3^-}$ motifs. Only species involved in these interactions are shown.

Description of the structures of complexes 11–13

$[NiX_2L_2]$ type complexes. By changing the metal-to-ligand ratio to 1 : 1, the reactions resulted in complexes **11–13** with $X^- = Cl^-$ (**11**), Br^- (**12**), and NO_2^- (**13**). Attempts to isolate the analogous compounds with HL′ did not yield any diffraction-quality crystals. The metal centre in complexes **11** and **12** is coordinated by two pyridine-type nitrogen donor atoms from each ligand and the two terminal halides, resulting in a distorted tetrahedral N_2X_2 geometry. The two ligands in both complexes are mutually arranged in a *syn* fashion. Each complex is stabilized by two intramolecular π···π stackings, similar to those observed in complexes **1–10**, and have a similar conformation, the main differences being in the orientation of the phenyl rings not involved in the intramolecular π···π pattern. However, small differences in the *molecular* structure can result in noticeable changes in the *crystal packing*.[25] Indeed, the supramolecular organization of compound **11** is based on weak intermolecular C–H···Cl and C–H···π interactions forming layers, which are further linked by similar interactions and π···π stackings in a 3D structure in the *Pbcn* space group (Fig. 5, left). The same type of bonding (C–H···Br and C–H···π) is also present in compound **12** but no intermolecular π···π stackings form, resulting in a different crystal packing ($I4_1cd$ space group). This difference is likely due to a combination of several effects, including the longer Ni–Br distance (compared to Ni–Cl) and the different number of C–H···X (X = Cl, Br) interactions formed by the coordinated halogeno ions (up to two bonds for compound **11** and up to four for **12**).

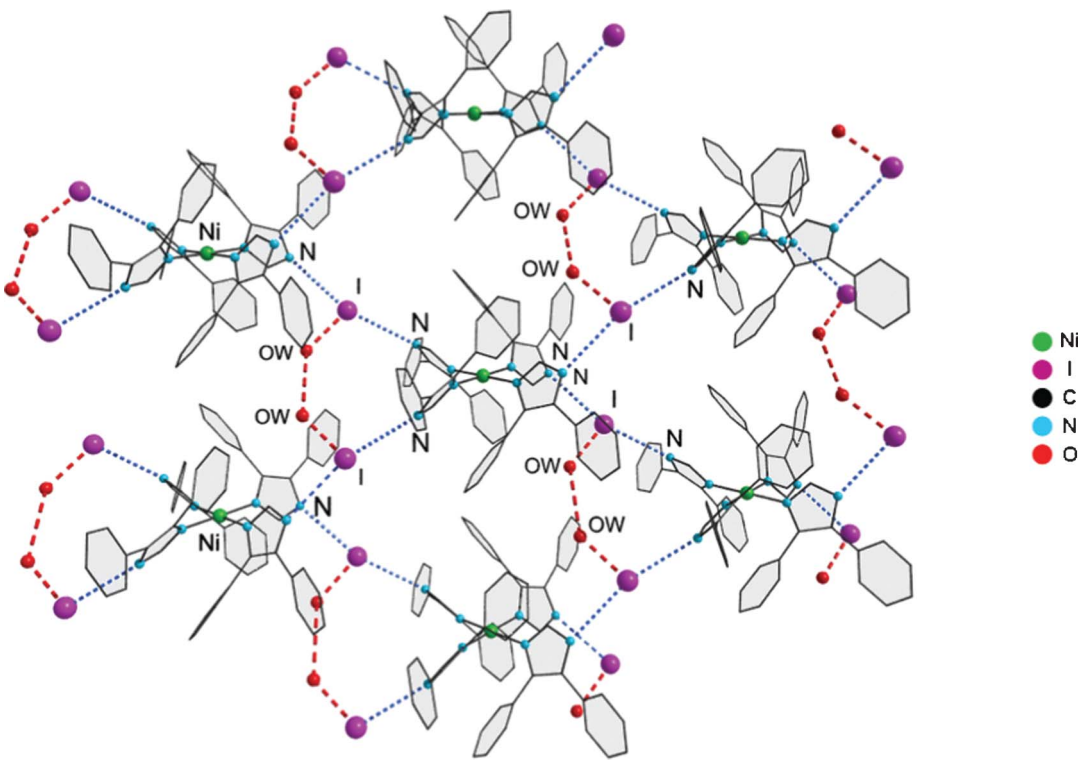

Fig. 4 Part of the structure of compound **8**. The rigid $[Ni(HL')_4]^{2+}$ cations are surrounded by clusters of iodide counterions and water solvent molecules (red dashed lines) and form layers *via* strong N–H···I^- motifs (blue dashed lines). The H-atoms and the acetone molecules of the clusters, linking the layers in a 3D structure, have been omitted. Non-carbon atoms are drawn as spheres of arbitrary radii.

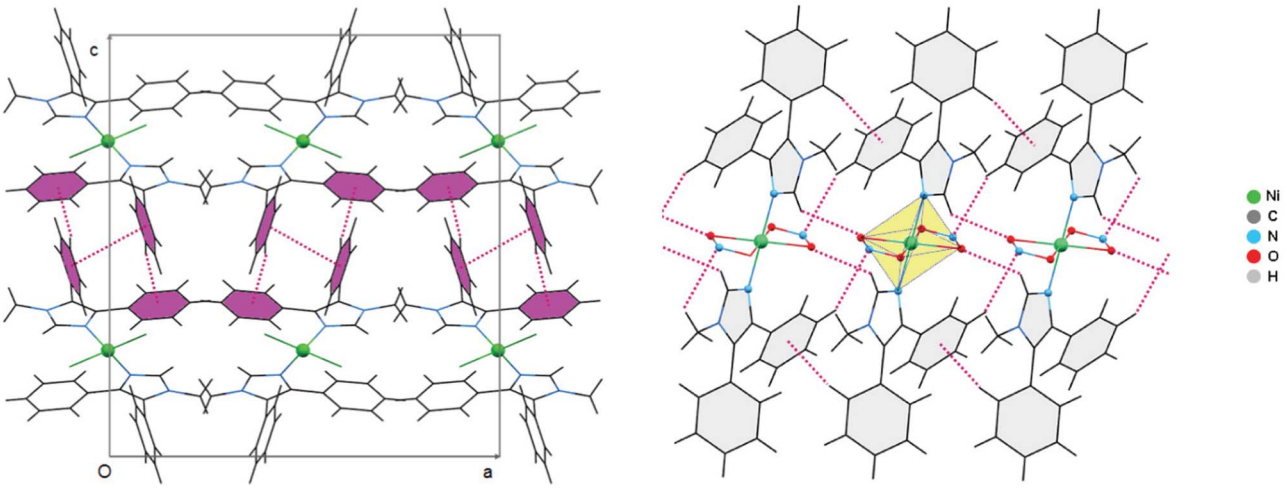

Fig. 5 (Left) Projection of compound **11** on the *ac* plane. The intermolecular π···π and C–H···π interactions connecting the layers (which are parallel to the *ab* plane) in a 3D structure are coloured violet. (Right) Tapes in the crystal structure of compound **13** formed by weak C–H···O, C–H···N and C–H···π interactions (shown in red dashed lines). The octahedral polyhedron around the nickel atoms is coloured yellow.

In compound **13**, the two nitrite ions, acting as bidentate chelating ligands, coordinate to the nickel through the four oxygen atoms while the two imidazole ligands, through their pyridine-type nitrogen atoms, act as axial ligands allowing the nickel cation to acquire its preferred octahedral coordination (Fig. 5, right). The *trans* disposition of the ligands does not favour the formation of the characteristic intramolecular π···π motif observed so far in all square planar (**1–10**) and tetrahedral structures (**11**, **12**). However, this allows the phenyl rings to rotate so that the structure assembles in a 'tighter' supramolecular packing. This is reflected in a higher packing index[26] (71.5%) for **13**, as compared to 67.2% for **11** and 67.3% for **12**. In terms of supramolecular organization, the complexes are connected *via* weak C–H···O, C–H···N and C–H···π interactions into tapes along the *a* axis which are further linked by C–H···π interactions into layers parallel to the *ab* plane.

Conclusions

The study of a series of Ni(II) complexes with a variety of coordination motifs has disclosed interesting features of their 2D and 3D supramolecular architectures. In terms of molecular organization, use of the L and HL′ ligands has resulted in square planar $[NiL_4]^{2+}$ (**1–5**) and $[Ni(HL')_4]^{2+}$ (**6–10**) complexes in accordance to Crystal Field Theory for medium-field bulky ligands, in tetrahedral coordination in $[NiX_2L_2]$ complexes for weak-field halogeno ligands [X = Cl (**11**), Br (**12**)], and octahedral in the $[Ni(NO_2)_2L_2]$ complex (**13**) due to the large CFSE for this geometry.

The rigid $[NiL_4]^{2+}$ and $[Ni(HL')_4]^{2+}$ cations in compounds **1–10**, stabilized by a characteristic motif of four intramolecular π···π stacking interactions, seem to have an impact on the supramolecular organization by adopting a structure-directing role. Regardless of the ligand (L or HL′) used, each structure is organized around the rigid and bulky $[NiL_4]^{2+}$ or $[Ni(HL')_4]^{2+}$ cations *via* interactions with surrounding counterion/solvent clusters in each individual structure. The components of the clusters, *i.e.* OH^-/H_2O (**1**), $[NiCl_4]^{2-}$/EtOH (**2**), Br^-/H_2O (**3**), NO_3^-/MeOH (**4**), ClO_4^-/Me_2CO (**5**), Cl^-/H_2O (**6**), Br^-/MeCN (**7**), $I^-/Me_2CO/H_2O$ (**8**), NO_3^-/EtOH/H_2O (**9**), and ClO_4^-/Me_2CO (**10**), are held tightly together by strong or weak hydrogen bonds. In particular, the water molecules within the clusters of **1**, **3**, **6**, **8** and **9** seem to exert a structural role towards the organization of the crystalline structures, rather than simply being present as co-crystallized solvent molecules.

The ligands selected allowed the implementation of a designed bonding scheme, including classical and weak hydrogen bonds, as well as weak π-system interactions. In particular, the assembly of the $[NiL_4]^{2+}$ cations with the counterion/solvent clusters in compounds **1–5** is accomplished through a network of weak, yet steadily occurring in all structures, C–H···O/Cl/Br^-, π···π and C–H···π interactions, demonstrating the strength of their collaborative action and leading to well-organized 2D and 3D structures. On the other hand, the system of interactions responsible for the construction of the crystalline structures with HL′ (compounds **6–10**) is clearly hierarchic. At the first level of organization, the counterion/solvent clusters provide the appropriate acceptors to generate, with the NH donor groups of the $[Ni(HL')_4]^{2+}$ cations, strong N–H···$Cl^-/Br^-/I^-$/O motifs (supramolecular synthons) present in all crystalline structures. Then, similarly to compounds **1–5**, weak interactions contribute to the 3D expansion of the structures.

Complexes **1–10** have no counterparts in Co^{II} and Zn^{II} chemistry,[18] due to the inability of the latter two metal ions to form square planar structures. The molecular structures of **11** and **12** are similar to those of $[MX_2L_2]$ (M = Co, Zn; X = Cl, Br). We were unable to observe polymorphs of **11**, in contrast to $[CoCl_2L_2]$ and $[ZnCl_2L_2]$ where two polymorphs were identified for each complex. The supramolecular structures of **12**, $[CoBr_2L_2]$ and $[ZnBr_2L_2]$[18] are isomorphous crystallizing in the $I4_1cd$ space group. Octahedral $[M(NO_2)_2L_2]$ complexes are known in Co^{II} and Zn^{II} chemistry.[18] However, the two L ligands are mutually *cis* in contrast to their *trans* orientation in **13**. As a result, their supramolecular structures differ.

We are currently expanding our research efforts to prepare analogous species with copper(II), a 3d-metal ion whose coordination preferences differ from those of nickel(II), to check the impact of the metal coordination on the composition of the building blocks and their subsequent supramolecular organization.

Experimental

Materials and instruments

Chemicals (reagent grade) were purchased from Merck and Alfa Aesar. All manipulations were performed under aerobic conditions using materials and solvents as received; water was distilled in-house. The ligand 1-methyl-4,5-diphenylimidazole (L) was synthesized as already described in the literature.[27] Microanalyses (C, H, N) were performed by the University of Ioannina (Greece) Microanalytical Laboratory using an EA 1108 Carlo Erba analyzer. IR spectra were recorded on a Perkin-Elmer PC 16 FT-IR spectrometer with samples prepared as KBr pellets (Fig. S3, ESI†).

Safety note: Perchlorate salts are potentially explosive; such compounds should be synthesized and used in small quantities, and treated with utmost care at all times.

Synthesis of $[NiL_4](OH)_2\cdot H_2O$ ($1\cdot H_2O$). This compound was synthesized by a solvothermal reaction of L (0.059 g, 0.25 mmol) and $NiCl_2\cdot 6H_2O$ (0.024 g, 0.10 mmol) in MeCN (8 ml). The resultant solution was heated at 100 °C in a Teflon-lined stainless steel autoclave for 3 days. The reaction system was then slowly cooled (5 °C h^{-1}) to room temperature. The reaction solution was filtered. Upon slow evaporation of the filtrate, light green prismatic crystals of $\mathbf{1}\cdot H_2O$ were obtained after 11 days in a 60% yield (based on L). Anal. Calcd for $\mathbf{1}\cdot H_2O$: C, 73.35; H, 5.77; N, 10.69%. Found: C, 73.44; H, 5.63; N, 10.58%. Selected IR bands (KBr, cm^{-1}): 3470 sb, 3420 mb, 1602 w, 1527 m, 1504 m, 1483 m, 1441 s, 1365 w, 1248 w, 1194 m, 1157 w, 1068 m, 1020 m, 985 w, 951 w, 793 w, 769 s, 748 w, 701 s, 650 s, 587 w, 517 w, 435 w.

Synthesis of $[NiL_4][NiCl_4]\cdot 2EtOH$ ($2\cdot 2EtOH$). A solution of L (0.375 g, 1.60 mmol) and $NiCl_2\cdot 6H_2O$ (0.095 g, 0.40 mmol) in EtOH/TEOF (15 ml/3 ml) was refluxed for 1 h. The reaction solution was filtered. Upon slow evaporation of the filtrate, light green prismatic crystals of $\mathbf{2}\cdot 2EtOH$ were obtained after 3 days in a 40% yield [based on nickel(II)]. Anal. Calcd for **2**: C, 64.25; H, 4.71; N, 9.36%. Found: C, 64.34; H, 4.83; N, 9.29%. Selected IR bands (KBr, cm^{-1}): 3420 sb, 3114 w, 1602 m, 1578 w, 1528 s, 1508 m, 1482 m, 1444 m, 1196 m, 1156 w, 1072 m, 1018 m, 794 m, 774 s, 700 s, 650 m, 516 w, 402 w.

Synthesis of $[NiL_4]Br_2\cdot 3.4H_2O$ ($3\cdot 3.4H_2O$). A solution of L (0.375 g, 1.60 mmol) and $NiBr_2\cdot 3H_2O$ (0.087 g, 0.40 mmol) in CH_2Cl_2/TEOF (20 ml/3 ml) was refluxed for 1 h. The reaction solution was filtered. Upon slow evaporation of the filtrate, yellow prismatic crystals of $\mathbf{3}\cdot 3.4H_2O$ were obtained after 1 day in a 60% yield [based on nickel(II)]. Anal. Calcd for $\mathbf{3}\cdot 3.4H_2O$: C, 63.54; H, 5.16; N, 9.26%. Found: C, 63.41; H, 5.02; N, 9.34%. Selected IR bands (KBr, cm^{-1}): 3418 mb, 3112 w, 1600 w, 1528 m, 1506 m, 1482 m, 1442 m, 1366 w, 1250 w, 1194 m, 1158 w, 1070 m, 1020 m, 986 w, 952 w, 794 w, 772 s, 750 w, 700 s, 648 s, 588 w, 514 wb, 436 w.

Synthesis of $[NiL_4](NO_3)_2\cdot 2.8MeOH$ ($4\cdot 2.8MeOH$). A solution of L (0.293 g, 1.25 mmol) and $Ni(NO_3)_2\cdot 6H_2O$ (0.145 g, 0.50 mmol) in MeOH (25 ml) was stirred for 30 min. The reaction solution was filtered. Upon slow evaporation of the filtrate, yellow prismatic crystals of $\mathbf{4}\cdot 2.8MeOH$ were obtained after 7 days in a 30% yield (based on L). Anal. Calcd for **4**: C, 68.64; H, 5.04; N, 12.51%. Found: C, 68.56; H, 4.91; N, 12.62%. Selected IR bands (KBr, cm^{-1}): 3134 w, 1654 w, 1528 m, 1484 w, 1384 s, 1196 w, 1072 m, 1020 m, 986 w, 724 w, 698 s, 670 w, 514 w.

Synthesis of $[NiL_4](ClO_4)_2\cdot Me_2CO$ ($5\cdot Me_2CO$). A solution of L (0.375 g, 1.6 mmol) and $Ni(ClO_4)_2\cdot 6H_2O$ (0.146 g, 0.40 mmol) in Me_2CO (25 ml) was stirred for 30 min. The reaction solution was filtered. Upon slow evaporation of the filtrate, yellow prismatic crystals of $\mathbf{5}\cdot Me_2CO$ were obtained after 4 days in a *ca.* 60% yield [based on nickel(II)]. Anal. Calcd for **5**: C, 64.33; H, 4.72; N, 9.37%. Found: C, 64.42; H, 4.86; N, 9.24%. Selected IR bands (KBr, cm^{-1}): 3138 m, 3050 w, 1602 m, 1528 s, 1484 m, 1444 m, 1194 m, 1098 vs, 1018 m, 782 m, 774 m, 746 m, 696 s, 648 m, 624 s.

Synthesis of $[Ni(HL')_4][NiCl_2(HL')_2]_2Cl_2\cdot 1.35H_2O$ ($6\cdot 1.35H_2O$). This compound was synthesized by the solvothermal reaction of HL′ (0.165 g, 0.75 mmol) and $NiCl_2\cdot 6H_2O$ (0.071 g, 0.30 mmol) in MeCN (8 ml). The reaction procedure was similar to that of $\mathbf{1}\cdot H_2O$. The reaction solution was stored in a closed flask at room temperature. Blue prismatic crystals of $\mathbf{6}\cdot 1.35H_2O$ were obtained after 2 days in a 30% yield (based on HL′). Anal. Calcd for $\mathbf{6}\cdot 1.35H_2O$: C, 66.45; H, 4.55; N, 10.33%. Found: C, 66.57; H, 4.39; N, 10.19%. Selected IR bands (KBr, cm^{-1}): 3134 w, 3064 w, 1508 m, 1458 w, 1398 w, 1374 w, 1072 w, 1026 w, 978 w, 764 s, 724 w, 694 s, 648 m, 494 w.

Synthesis of $[Ni(HL')_4]Br_2\cdot 4.7MeCN$ ($7\cdot 4.7MeCN$). A solution of HL′ (0.138 g, 0.63 mmol) and $NiBr_2\cdot 3H_2O$ (0.055 g, 0.25 mmol) in MeCN (20 ml) was stirred for 30 min. The colourless solution was left to slowly evaporate at low temperature (5 °C). Yellow prismatic crystals of $\mathbf{7}\cdot 4.7MeCN$ were obtained after 3 days in a 40% yield (based on HL′). Anal. Calcd for **7**: C, 65.53; H, 4.40; N, 10.19%. Found: C, 65.41; H, 4.29; N, 10.27%. Selected IR bands (KBr, cm^{-1}): 3060 mb, 1604 w, 1510 s, 1486 m, 1442 m, 1314 w, 1294 w, 1158 w, 1132 m, 1072 m, 958 w, 764 s.

Synthesis of $[Ni(HL')_4]I_2\cdot 2Me_2CO\cdot 0.8H_2O$ ($8\cdot 2Me_2CO\cdot 0.8H_2O$). A solution of HL′ (0.275 g, 1.25 mmol) and $NiI_2\cdot 6H_2O$ (0.210 g, 0.50 mmol) in Me_2CO (25 ml) was refluxed for 1 h. The reaction solution was filtered. The resultant green solution was layered with *n*-hexane (50 ml) to produce dark orange prismatic crystals of $\mathbf{8}\cdot 2Me_2CO\cdot 0.8H_2O$ in 6 days; yield *ca.* 40% (based on HL′). Anal. Calcd for $\mathbf{8}\cdot 0.8H_2O$: C, 60.32; H, 4.13; N, 9.37%. Found: C, 60.24; H, 4.01; N, 9.26%. Selected IR bands (KBr, cm^{-1}): 3068 mb, 1604 m, 1590 w, 1508 m,

1490 m, 1444 m, 1158 w, 1026 w, 982 w, 914 w, 764 s, , 696 s, 648 m, 564 w, 494 w.

Synthesis of $[Ni(HL')_4](NO_3)_2{\cdot}2EtOH{\cdot}2H_2O$ ($9{\cdot}2EtOH{\cdot}2H_2O$). A solution of HL′ (0.138 g, 0.63 mmol) and $Ni(NO_3)_2{\cdot}6H_2O$ (0.073 g, 0.25 mmol) in EtOH/TEOF (20 ml/3 ml) was refluxed for 1 h. The reaction solution was filtered. Upon slow evaporation of the filtrate, yellow prismatic crystals of $9{\cdot}2EtOH{\cdot}2H_2O$ were obtained after 1 day in a 40% yield (based on HL′). Anal. Calcd for $9{\cdot}2H_2O$: C, 65.52; H, 4.76; N, 12.73%. Found: C, 65.43; H, 4.62; N, 12.86%. Selected IR bands (KBr, cm^{-1}): 3112 w, 3064 w, 1604 m, 1510 w, 1488 m, 1444 m, 1384 s, 1340 m, 1318 m, 1156 w, 1134 m, 1072 m, 1046 m, 822 w, 764 s, 694 s, 648 m, 580 m, 402 w.

Synthesis of $[Ni(HL')_4](ClO_4)_2{\cdot}2.8Me_2CO$ ($10{\cdot}2.8Me_2CO$). A solution of HL′ (0.350 g, 1.60 mmol) and $Ni(ClO_4)_2{\cdot}6H_2O$ (0.146 g, 0.40 mmol) in Me_2CO (20 ml) was stirred for 30 min. The reaction solution was filtered. The resultant orange solution was layered with Et_2O/*n*-hexane (20 ml/20 ml) to produce orange prismatic crystals of $10{\cdot}2.8Me_2CO$ in 2 days; yield *ca.* 60% [based on nickel(II)]. Anal. Calcd for **10**: C, 63.28; H, 4.24; N, 9.84%. Found: C, 63.13; H, 4.11; N, 9.72%. Selected IR bands (KBr, cm^{-1}): 3146 w, 3054 w, 1604 w, 1526 m, 1483 m, 1442 w, 1194 m, 1098 vs, 1016 m, 789 m, 778 w, 742 m, 694 s, 648 m, 628 s.

Synthesis of $[NiCl_2L_2]$ (11). A solution of L (0.094 g, 0.40 mmol) and $NiCl_2{\cdot}6H_2O$ (0.095 g, 0.40 mmol) in EtOH (20 ml) was stirred for 30 min. The reaction solution was filtered. Upon slow evaporation of the filtrate, violet prismatic crystals of **11** were obtained after 20 days in a 30% yield (based on L). Anal. Calcd for **11**: C, 64.25; H, 4.71; N, 9.36%. Found: C, 64.38; H, 4.54; N, 9.22%. Selected IR bands (KBr, cm^{-1}): 3384 sb, 3134 w, 1636 w, 1602 w, 1544 w, 1516 m, 1480 m, 1442 m, 1366 w, 1318 w, 1192 m, 1072 m, 980 w, 916 w, 792 m, 770 s, 698 s, 648 m, 584 w, 456 w.

Synthesis of $[NiBr_2L_2]$ (12). A solution of L (0.087 g, 0.40 mmol) and $NiBr_2{\cdot}3H_2O$ (0.087 g, 0.40 mmol) in CH_2Cl_2/TEOF (20 ml/3 ml) was refluxed for 1 h. The reaction procedure was similar to that of $3{\cdot}3.4H_2O$. Dark blue needles of **12** were obtained after 17 days in a 40% yield (based on L). Anal. Calcd for **12**: C, 55.93; H, 4.11; N, 8.15%. Found: C, 55.71; H, 3.94; N, 8.29%. Selected IR bands (KBr, cm^{-1}): 3414 sb, 3114 w, 1602 m, 1576 w, 1528 s, 1482 m, 1444 m, 1420 m, 1404 w, 1326 w, 1196 m, 1154 w, 1072 m, 1044 w, 1018 m, 912 w, 794 s, 774 s, 750 m, 724 m, 702 sh, 694 s, 650 m, 588 w, 436 w.

Synthesis of $[Ni(NO_2)_2L_2]$ (13). $Ni(ClO_4)_2{\cdot}6H_2O$ (0.110 g, 0.30 mmol) and L (0.176 g, 0.75 mmol) were dissolved in MeOH (15 ml). To the resulting green solution, $NaNO_2$ (0.052 g, 0.75 mmol) in MeOH (10 ml) was added dropwise. The reaction solution was filtered. Upon slow evaporation of the filtrate, light green rods of **13** appeared after 5 days in a 40% yield [based on nickel(II)]. Anal. Calcd for **13**: C, 62.06; H, 4.55; N, 13.57%. Found: C, 62.21; H, 4.36; N, 13.41%. Selected IR bands (KBr, cm^{-1}): 3060 w, 1602 w, 1524 m, 1508 sh, 1458 w, 1442 w, 1402 w, 1374 w, 1330 w, 1298 w, 1262 w, 1214 s, 1198 sh, 1178 sh, 1126 w, 1020 w, 826 w, 784 m, 774 sh, 692 m, 650 m, 580 w.

X-ray crystallography

Single-crystals covered with paratone-N oil were mounted on the tip of glass fibres or were scooped up in cryo-loops at the end of a copper pin. X-ray diffraction data were collected (ω-scans) with an Xcalibur-3 and a SuperNova A Oxford Diffraction diffractometers under a flow of nitrogen gas at 100(2) K using Mo-Kα radiation (λ = 0.7107 Å) except for compounds **5** and **13** where Cu-Kα (λ = 1.5418 Å) was used. Data were collected and processed by the CRYSALIS CCD and RED software,[28] respectively, and the reflection intensities were corrected for absorption by the multiscan method. All structures were solved using SIR92[29] and SHELXS-97[30] and refined by full-matrix least-squares on F^2 with SHELXL-97.[31] All non-H atoms were refined anisotropically, and carbon-bound H-atoms were introduced at calculated positions and allowed to ride on their carrier atoms. Non-routine aspects of structure refinement are as follows: All imidazole H-atoms on the pyrrolic type N1 atom of the HL′-containing compounds, as well as the hydroxyl H-atoms of solvents in compounds **1** (H_2O), **4** (MeOH), and **2** and **9** (EtOH) were located in difference Fourier maps and refined isotropically applying soft distance restraints (DFIX). The structure of **1** was refined as a merohedral twin (with an 97 : 3 twin components ratio), the structure of **5** as a twin by inversion (51 : 49 twin ratio), and the structures of **10** and **13** as non-merohedral twins (64 : 36 and 70 : 30 twin ratio, respectively). The bromide (in **3** and **7**) and iodide (in **8**) counterions are disordered and have been modelled over two orientations, while the chloride counterion and a lattice water molecule in structure **6** are disordered over two sites forming two mixed Cl^-/H_2O sites as was concluded after competitive and detailed refinement. The crystal structures of **1** and **9** contain a small area of disordered solvent (water), and the structure of **5** a highly disordered perchlorate counterion.

Attempts to model them with a chemically reasonable geometry were unsuccessful; therefore, the SQUEEZE procedure of PLATON[32] was employed to remove the contribution of the electron density associated with those molecules from the intensity data. However, the role of the disordered perchlorate in the supramolecular organization of **5** has been taken into account using a structural model prior to deletion. Geometric/crystallographic calculations were carried out using PLATON,[32] OLEX2,[33] X-Seed[34] and WINGX[35] packages; molecular/packing graphics were prepared with DIAMOND[36] and MERCURY.[37] Crystallographic data collection and refinement parameters are listed in Table 2.

Acknowledgements

This work was supported by the Research Committee of the University of Patras, Greece (K. Caratheodory program, Grant No. C.585 to VN). AJT thanks the Cyprus Research Promotion Foundation Grant "ΑΝΑΒΑΘΜΙΣΗ/ΠΑΓΙΟ/0308/12" which is co-funded by the Republic of Cyprus and the European Regional Development Fund. We also thank graduate student Despoina Dermitzaki for performing some preliminary experiments.

Table 2 Crystal data and structure refinement summary for compounds **1–13**

Compound	**1**	**2**	**3**	**4**	**5**	**6**	**7**	**8**	**9**	**10**	**11**	**12**	**13**
Chemical formula	$C_{64}H_{56}N_8Ni\cdot 2(OH)\cdot H_2O$	$C_{64}H_{56}N_8Ni\cdot NiCl_4\cdot 2(C_2H_5OH)$	$C_{64}H_{56}N_8Ni\cdot 2Br\cdot 3.4(H_2O)$	$C_{64}H_{56}N_8Ni\cdot 2(NO_3)\cdot 2.8(CH_3OH)$	$C_{64}H_{56}N_8Ni\cdot 2(ClO_4)\cdot CH_3COCH_3$	$C_{60}H_{48}N_8Ni\cdot 2(C_{30}H_{24}Cl_2\cdot N_4Ni)\cdot 2Cl\cdot 1.35(H_2O)$	$C_{60}H_{48}N_8Ni\cdot 2Br\cdot 4.7(CH_3CN)$	$C_{60}H_{48}N_8Ni\cdot 2I\cdot 2(CH_3COCH_3)\cdot 0.8(H_2O)$	$C_{60}H_{48}N_8Ni\cdot 2(NO_3)\cdot 2(C_2H_5OH)\cdot 2(H_2O)$	$C_{60}H_{48}N_8Ni\cdot 2(ClO_4)\cdot 2.8(CH_3COCH_3)$	$C_{32}H_{28}Cl_2N_4Ni$	$C_{32}H_{28}Br_2N_4Ni$	$C_{32}H_{28}N_6NiO_4$
Formula weight/ g mol^{-1}	1047.91	1288.52	1216.95	1209.62	1252.86	2175.28	1292.55	1324.14	1191.96	1301.29	598.19	687.11	619.31
Crystal system	Orthorhombic	Orthorhombic	Orthorhombic	Monoclinic	Orthorhombic	Triclinic	Triclinic	Orthorhombic	Orthorhombic	Monoclinic	Orthorhombic	Tetragonal	Triclinic
Space group	*Aba*2	*Aba*2	*Aba*2	$P2_1/n$	$Pna2_1$	$P\bar{1}$	$P\bar{1}$	*Aba*2	*Iba*2	*Pc*	*Pbcn*	$I4_1cd$	$P\bar{1}$
a/Å	11.4027(3)	11.6264(2)	11.4808(2)	11.1951(2)	23.7034(5)	15.7526(5)	12.2832(4)	23.8271(7)	11.4752(3)	13.1954(7)	17.4689(4)	28.6711(3)	6.0809(3)
b/Å	23.4885(6)	24.3482(3)	23.4663(4)	29.4448(4)	11.7726(3)	19.9434(7)	15.2035(6)	11.3058(4)	22.9510(5)	23.8866(10)	8.7125(2)	28.6711(3)	7.3878(5)
c/Å	22.6238(5)	22.2375(3)	22.5673(4)	18.0834(3)	22.0772(7)	19.9541(8)	19.4459(6)	23.1922(8)	22.8593(5)	11.2041(7)	18.7322(4)	14.0797(2)	16.0562(10)
α (°)	90	90	90	90	90	116.937(4)	69.188(3)	90	90	90	90	90	100.554(6)
β (°)	90	90	90	96.759(2)	90	103.576(3)	82.117(2)	90	90	114.105(7)	90	90	98.892(5)
γ (°)	90	90	90	90	90	93.729(3)	68.905(3)	90	90	90	90	90	94.548(5)
V/Å^3	6059.4(3)	6295.0(2)	6079.9(2)	5919.5(2)	6160.6(3)	5325.2(3)	3166.9(2)	6247.6(4)	6020.4(2)	3223.5(3)	2851.0(1)	11 574.0(2)	696.3(1)
Z, *Z*′	4, 05	4, 0.5	4, 0.5	4, 1	4, 1	2, 1	2, 1	4, 0.5	4, 0.5	2, 1	4, 0.5	16, 1	1, 0.5
T/K	100(2)	100(2)	100(2)	100(2)	100(2)	100(2)	100(2)	100(2)	100(2)	100(2)	100(2)	100(2)	100(2)
Radiation type, *μ*/mm^{-1}	Mo-Kα, 0.370	Mo-Kα, 0.820	Mo-Kα, 1.685	Mo-Kα, 0.396	Cu-Kα, 1.781	Mo-Kα, 0.735	Mo-Kα, 1.620	Mo-Kα, 1.349	Mo-Kα, 0.390	Mo-Kα, 0.450	Mo-Kα, 0.897	Mo-Kα, 3.461	Cu-Kα, 1.423
No. of reflections measured	25 119	27 016	19 272	50 939	14 444	58 902	55 461	13 235	5714	25 177	23 736	49 601	2135
No. of independent reflections	5996	8297	4785	14 953	8850	21 984	15 930	6040	5714	25 177	3777	7673	2135
Final R_1 values ($I > 2\sigma(I)$)	0.0489	0.0372	0.0780	0.0490	0.0573	0.0454	0.0443	0.0423	0.0434	0.0875	0.0328	0.0251	0.0725
Final w$R(F^2)$ values ($I > 2\sigma(I)$)	0.1211	0.0908	0.2007	0.1029	0.1542	0.0784	0.0858	0.1158	0.1067	0.2353	0.0608	0.0454	0.1905
Final R_1 values (all data)	0.0642	0.0452	0.0933	0.0937	0.0624	0.0986	0.0892	0.0463	0.0582	0.0955	0.0665	0.0334	0.0742
Final w$R(F^2)$ values (all data)	0.1250	0.0930	0.2135	0.1101	0.1606	0.0863	0.0903	0.1183	0.1114	0.2476	0.0653	0.0461	0.1910
Goodness of fit on F^2	0.989	0.983	1.037	0.927	1.024	0.940	0.921	1.010	0.996	1.100	0.846	0.902	1.065
$\Delta\rho_{max}$ and $\Delta\rho_{min}$/e Å^{-3}	0.803, −0.410	0.600, −0.313	1.321, −1.185	0.788, −0.568	0.557, −0.553	0.932, −0.486	0.935, −0.890	1.074, −0.587	0.971, −0.490	0.956, −0.879	0.356, −0.324	0.515, −0.635	1.055, −0.673

References

1 (*a*) E. C. Constable, *Angew. Chem., Int. Ed. Engl.*, 1991, **30**, 1450; (*b*) R. Krämer, J.-M. Lehn and A. Marquis-Rigault, *Proc. Natl. Acad. Sci. U. S. A.*, 1993, **90**, 5394; (*c*) C. B. Aakeröy, *Acta Crystallogr., Sect. B: Struct. Sci.*, 1997, **B53**, 569; (*d*) A. Albrecht, *Naturwissenschaften*, 2007, **94**, 951; (*e*) E. C. Constable, G. Q. Zhang, C. E. Housecroft and J. A. Zampese, *CrystEngComm*, 2011, **13**, 6864.

2 (*a*) A. J. Blake, N. R. Champness, P. Hubberstey, W. S. Li, M. A Withersby and M. Schröder, *Coord. Chem. Rev.*, 1999, **183**, 117; (*b*) R. Robson, *Dalton Trans.*, **2000**, 3735; (*c*) B. Moulton and M. J. Zaworotko, *Chem. Rev.*, 2001, **101**, 1629.

3 (*a*) J.-M. Lehn, in *Supramolecular Chemistry. Concepts and Perspectives*, Wiley-VCH, Weinheim, 1995; (*b*) C. B. Aakeröy, N. R. Champness and C. Janiak, *CrystEngComm*, 2010, **12**, 22; (*c*) D. Braga and F. Grepioni, *Acc. Chem. Res.*, 2000, **33**, 601; (*d*) A. D. Burrows, R. W. Harrington, M. F. Mahon and S. J. Teat, *CrystEngComm*, 2005, **7**, 388; (*e*) A. Das, S. R. Choudhury, C. Estarellas, B. Dey, A. Frontera, J. Hemming, M. Helliwell, P. Gamez and S. Mukhopadhyay, *CrystEngComm*, 2011, **13**, 4519.

4 (*a*) J. W. Steed, J. L. Atwood, in *Supramolecular Chemistry*, Wiley, Chichester, 2009; (*b*) A. Dey, N. N. Pati and G. R. Desiraju, *CrystEngComm*, 2006, **8**, 751.

5 (*a*) G. R. Desiraju, T. Steiner, in *The Weak Hydrogen Bond In Structural Chemistry and Biology*, Oxford University Press/IUCr, 2001; (*b*) M. Simard, D. Su and J. D. Wuest, *J. Am. Chem. Soc.*, 1991, **113**, 4696; (*c*) M. J. Zaworotko, *Cryst. Growth Des.*, 2007, **7**, 4; (*d*) R. E. Meléndez and A. D. Hamilton, *Top. Curr. Chem.*, 1998, **198**, 97; (*e*) C. B. Aakeröy and A. M. Beatty, *Aust. J. Chem.*, 2001, **54**, 409; (*f*) A. D. Burrows, *Struct. Bonding*, 2004, **108**, 5595.

6 (*a*) C. Janiak, *J. Chem. Soc., Dalton Trans.*, 2000, 3885; (*b*) M. O. Sinnokrot and C. D. Sherrill, *J. Am. Chem. Soc.*, 2004, **126**, 7690; (*c*) C. Biswas, M. G. B. Drew, D. Escudero, A. Frontera and A. Ghosh, *Eur. J. Inorg. Chem.*, 2009, 2238; (*d*) S. R. Choudhury, B. Dey, S. Das, A. Robertazzi, A. D. Jana, C. Y. Chen, H. M. Lee, P. Gamez and S. Mukhopadhyay, *Dalton Trans.*, 2009, 7617; (*e*) J. K. Klosterman, Y. Yamauchi and M. Fujita, *Chem. Soc. Rev.*, 2009, **38**, 1714; (*f*) S. Grimme, *Angew. Chem., Int. Ed.*, 2008, **47**, 3430; (*g*) Z. J. Chen, A. Lohr, C. R. Saha-Möller and F. Würthner, *Chem. Soc. Rev.*, 2009, **38**, 564.

7 (*a*) F. Meyer, H. Kozlowski, in *Comprehensive Coordination Chemistry II*, ed. J. A. McCleverty and T. J. Meyer, Elsevier, Amsterdam, 2004, vol. **6**, pp. 247–554; (*b*) C. Papatriantafyllopoulou, T. C. Stamatatos, W. Wernsdorfer, S. J. Teat, A. J. Tasiopoulos, A. Escuer and S. P. Perlepes, *Inorg. Chem.*, 2010, **49**, 10486.

8 (*a*) M. Schröder, in *Encyclopedia of Inorganic Chemistry*, ed. R. B. King, Wiley, New York, 1994, vol. **5**, pp. 2392–2412; (*b*) G. Wilke, *Angew. Chem., Int. Ed. Engl.*, 1988, **27**, 185; (*c*) A. Dervisi, *Annu. Rep. Prog. Chem., Sect. A*, 2010, **106**, 223.

9 F. A. Cotton, G. Wilkinson, C.A. Murillo, M. Bochmann, in *Advanced Inorganic Chemistry*, Wiley, New York, 6th edn1999, pp. 835–846.

10 D. Nicholls, in *Complexes and First-Raw Transition Elements*, MacMillan Press, London, 1947, pp. 66–70.

11 H.-B Kraatz, N. Metzler-Nolte, in *Concepts and Models in Bioinorganic Chemistry*, Wiley-VCH, Weinheim, 2006.

12 J. M. Berg, S. J. Lippard, in *Principles of Bioinorganic Chemistry*, University Science Books, Mill Valley, California, 1994.

13 (*a*) S. Mukherjee, T. Weyhermüller, E. Bill and P. Chaudhuri, *Eur. J. Inorg. Chem.*, 2004, 4209; (*b*) A. Wojciechowska, M. Daszkiewicz, Z. Staszak, A. Trusz-Zdybek, A. Bieńko and A. Ozarowski, *Inorg. Chem.*, 2011, **50**, 11532; (*c*) L. F. Ma, X. Q. Li, L. Y. Wang and H. W. Hou, *CrystEngComm*, 2011, **13**, 4625; (*d*) D. Dobrzyńska, L. B. Jerzykiewicz, M. Duczmal, A. Wojciechowska, K. Jabłońska, J. Palus and A. Ozarowski, *Inorg. Chem.*, 2006, **45**, 10479.

14 (*a*) C. P. Raptopoulou, S. Paschalidou, A. A. Pantazaki, A. Terzis, S. P. Perlepes, T. Lialiaris, E. G. Bakalbassis, J. Mrozinski and D. A. Kyriakidis, *J. Inorg. Biochem.*, 1998, **71**, 15; (*b*) S. Zanias, G. S. Papaefstathiou, C. P. Raptopoulou, K. T. Papazisis, V. Vala, D. Zambouli, A. H. Kortsaris, D. A. Kyriakidis and T. F. Zafiropoulos, *Bioinorg. Chem. Appl.*, 2010, 10, Article ID 168030.

15 A. Hadzovic and D. Song, *Organometallics*, 2008, **27**, 1290.

16 K. A. Kounavi, C. Papatriantafyllopoulou, A. J. Tasiopoulos, S. P. Perlepes and V. Nastopoulos, *Polyhedron*, 2009, **28**, 3349.

17 K. A. Kounavi, J. Manos, A. J. Tasiopoulos, S. P. Perlepes and V. Nastopoulos, *Bioinorg. Chem. Appl.*, 2010, 7, Article ID 178034.

18 K. A. Kounavi, M. J. Manos, E. Moushi, A. A. Kitos, C. Papatriantafyllopoulou, A. J. Tasiopoulos and V. Nastopoulos, *Cryst. Growth Des.*, 2012, **12**, 429 and references therein.

19 (*a*) X.-J. Yang, F. Drepper, B. Wu, W.-H. Sun, W. Haehnel and C. Janiak, *Dalton Trans.*, 2005, 256; (*b*) K. Chłopek, E. Bill, T. Weyhermüller and K. Wieghardt, *Inorg. Chem.*, 2005, **44**, 7087.

20 Y. Gong, C. Hu, H. Li, W. Pan, X. Niu and Z. Pu, *J. Mol. Struct.*, 2005, **740**, 153.

21 (*a*) C. Brock and J. Dunitz, *Chem. Mater.*, 1994, **6**, 1118; (*b*) E. Pidcock and W. D. S. Motherwell, *Cryst. Growth Des.*, 2004, **4**, 611.

22 (*a*) M. Nishio, M. Hirota, Y. Umezawa, in *The C–H···π Interactions (Evidence, Nature and Consequences)*, Wiley, New York, 1998; (*b*) T. Ozawa, E. Tsuji, M. Ozawa, C. Handa, H. Mukaiyama, T. Nishimura, S. Kobayashi and K. Okazaki, *Bioorg. Med. Chem.*, 2008, **16**, 10311; (*c*) M. Nishio, Y. Umezawa, K. Honda, S. Tsuboyama and H. Suezawa, *CrystEngComm*, 2009, **11**, 1757.

23 C. H. Görbitz and H. P. Hersleth, *Acta Crystallogr., Sect. B: Struct. Sci.*, 2000, **B56**, 526.

24 S. Varughese and G. R. Desiraju, *Cryst. Growth Des.*, 2010, **10**, 4184.

25 G. R. Desiraju, *Acc. Chem. Res.*, 2002, **35**, 565.

26 A. I. Kitaigorodsky, in *Molecular Crystals and Molecules*, Academic Press, New York, 1973, p. p. 18.

27 J. McMaster, R. L. Beddoes, D. Collison, D. R. Eardley, M. Helliwell and C. D. Garner, *Chem.–Eur. J.*, 1996, **2**, 685.

28 *CrysAlis CCD and CrysAlis RED*, Oxford Diffraction Ltd, Abingdon, Oxford, UK, 2009.

29 A. Altomare, M. C. Burla, M. Camalli, G. Cascarano, C. Giacovazzo, A. Guagliardi and G. Polidori, *J. Appl. Crystallogr.*, 1994, **27**, 435.

30 G. M. Sheldrick, *SHELXS-97, Program for solution of crystal structures*, University of Göttingen, Germany, 1997.

31 G. M. Sheldrick, *SHELXL-97, Program for refinement of crystal structures*, University of Göttingen, Germany, 1997.

32 A. L. Spek, *Acta Crystallogr., Sect. A*, 1990, **46**, C34.

33 O. V. Dolomanov, L. J. Bourhis, R. J. Gildea, J. A. K. Howard and H. Puschmann, *J. Appl. Crystallogr.*, 2009, **42**, 339.

34 L. J. Barbour, *J. Supramol. Chem.*, 2001, **1**, 189.

35 L. J. Farrugia, *J. Appl. Crystallogr.*, 1999, **32**, 837.

36 K. Brandenburg, *DIAMOND: Program for Crystal and Molecular Structure Visualization*, Crystal Impact GbR, Bonn, Germany, 2011.

37 C. F. Macrae, P. R. Edgington, P. McCabe, E. Pidcock, G. P. Shields, R. Taylor, M. Towler and J. van de Streek, *J. Appl. Crystallogr.*, 2006, **39**, 453.

